Transactions of the Korean Nuclear Society Autumn Meeting
Gyeongju, Korea, October 29-30, 2015

Sensitivity analysis of penetration tube ejection model for APR 1400

Jaehoon Jung*, Sang Mo An, Kwang Soon Ha, Hwan Yeol Kim,
Korea Atomic Energy Research Institute (KAERI)
989-111 Daedeok-daero, Youseong-Gu, Daejeon 305-353, Republic of Korea
Email: jhjung@kaeri.re.kr

1. Introduction

Korean PWRs (Pressurized Water Reactors) have several ICI (In-Core Instrumentation) penetration tubes that penetrate the reactor vessel through the reactor bottom head. APR1400 has 61 ICI penetrations to monitor the in-core status [1]. The configuration of the ICI penetration tube at the center of APR1400 reactor bottom head is shown in Fig. 1. Even though the installation methodology of the penetrations varies from vendor design to design, they are attached to the inside of the reactor bottom head by a partial penetration weld as shown in Fig. 1. The penetrations are considered as the most vulnerable parts with respect to the reactor vessel failure when a severe accident like the Fukushima accident [2] occurs, since the melted core material (corium) relocated to the lower plenum of the reactor pressure vessel. Therefore, the determination of the failure modes and the timing at the lower head, such as the creep failure, the weld failure, the tube ejection, and a long term tube failure, is an important task under a given sever accident condition.

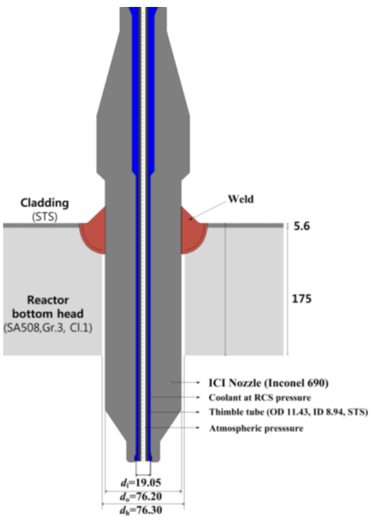

Fig. 1. Configuration of an ICI penetration tube

The penetration tube failure modes and mechanisms were identified [2]. Penetration tube failure can be divided into the two categories: tube ejection out of the vessel lower head and rupture of the penetration tube outside the vessel. Tube ejection begins with degrading the penetration tube weld strength to zero when the weld is exposed to higher temperatures that range up to melting and then overcoming any binding force in the a reactor vessel wall-penetration tube interface which results from differential thermal expansion of the tube and the reactor vessel. Tube rupture assumes that the debris bed has melted the instrument tube inside the reactor and melt migrates down into the tube to a location outside the vessel wall where a pressure rupture can occur, thus breaching the pressure boundary. So, the inside of reactor vessel pressure, the debris mass, the debris temperature, and the component materials can have an effect on the penetration tube failure modes. Furthermore, these parameters are inter-related. In these reasons, the failure model in the severe accident code requires a large amount of effort to increase the prediction of failure mode.

The present research focuses on the tube ejection mechanism for the APR 1400 in-core instrumentation penetration tubes. To get higher prediction for failure mode, the models which is included in the MAAP5 code [3] were modified. The models considered both the thermal and structural response of the vessel and lower head penetrations. A brief description of the failure models, along with assumptions used in the models, is provided. The validation works were performed using the KEARI’s experimental results from Verification of Ex-vessel corium STAbilization (VESTA) facility In addition, the sensitivity studies have been performed to reduce the difference between the analytic results and the experimental results.

2. Analysis model

When In the case of a severe accident like the Fukushima accident [2], the melted core material (corium) can be relocated to the lower plenum of the reactor pressure vessel, and attack the weld for holding the penetration tube inside the pressure vessel. As a result, the weld temperature sharply increases. The melted-off penetration tube would be exposed to both a substantial temperature gradient through the wall and a pressure difference which is between the reactor pressure vessel and the containment.

Figure 2 illustrates the free diagram of the ejection forces acting on a penetration tube. The pressure difference is supported by the shear stress in the weld as the following force balance.

$$(P_i + P_m - P_o)\frac{\pi d_o^2}{4} = \tau_w \pi d_o L_w \tag{1}$$

where L_w, d_0, P_m, P_o, P_i , and τ_w are the length of the weld, the outer diameter of the penetration tube, the pressure from the debris mass, the containment pressure, the pressure inside the reactor vessel and shear stress. The Shear stress is calculated from the pressure, pressure area, and shear area as follows, which is obtained from the Eq. 1.

$$\tau_w = \frac{(\mathrm{P_i} + \mathrm{P}_m - \mathrm{P}_o)\pi \mathrm{r_o^2}}{2\pi \mathrm{r_o L_w}} = \frac{(\mathrm{P_i} + \mathrm{P}_m - \mathrm{P}_o)\mathrm{r_o}}{2\mathrm{L_w}} \tag{2}$$

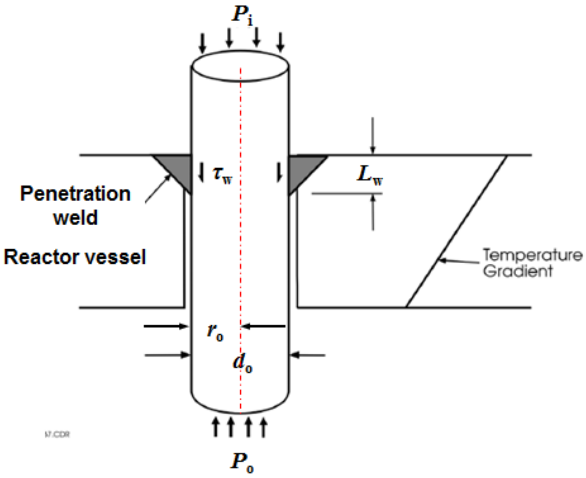

Fig. 2 Force acting on a vessel penetration [3]

When the molten corium attacks the weld and the reactor vessel wall, the weld melts due to the higher temperature of molten corium than the melting temperature of the weld. The weld length decreases as time goes on. However, the ablation effect doesn't consider in MAAP5 code. If the weld ablation effect was applied in the weld failure model, it becomes more conservative model because the decrease in the weld length leads to an increase in the shear stress as Eq. 3.

$$\tau_w = \frac{(\mathrm{P_i} + \mathrm{P}_m - \mathrm{P}_o)\pi \mathrm{r_o^2}}{2\pi \mathrm{r_o}\left(\mathrm{L_w} - W_{weld}t\right)} = \frac{(\mathrm{P_i} + \mathrm{P}_m - \mathrm{P}_o)\mathrm{r_o}}{2\left(\mathrm{L_w} - W_{weld}t\right)} \tag{3}$$

Whether the penetration can retain its integrity under the severe accident condition is determined by a comparison of the imposed shear stress and ultimate tensile strength. The ultimate tensile strength is strongly related to the temperature. It is known that the ultimate tensile strength dramatically decreases from near 600℃ to melting temperature [4]. In MAAP5 code, the ultimate tensile strength is determined by inputting the debris temperature since the weld was assumed as one lumped model. Although this assumption is very conservative, it is not a reasonable assumption because the weld temperature depends on each location. In the modified model, the yield stress of the weld is obtained the sum of the yield stress of each layer as follows [5]:

$$\sigma_{\mathrm{u}} = \frac{1}{L_w}\int_{W_{start}=0}^{\mathrm{W_{end}}=L_w} \sigma_{\mathrm{yp}}(T)dy \tag{4}$$

$$\sigma_{\mathrm{u}} > \sqrt{3}\tau_w \tag{5}$$

If the Eq.5 condition is satisfied, the weld failure does not occur, penetration ejection is precluded. However, once the weld failure occurs, the ability of the tube to bind in the vessel penetration hole should be considered to see if ejection could be restrained. In order to calculate the friction force (binding force), the following assumptions were used.

- The creep effects are negligible.
- The molten debris has traveled within a penetration to distances below the lower head.
- No support outside of the vessel resists tube ejection.
- The difference between the tube temperature at the inner surface and outer the surface is much smaller than the difference between the vessel inner and outer surface temperature.
- The tube-hole radial gap is constant.
- The expansion direction of the tube and hole is same.
- The material properties for high temperature; since the material properties are not always available for elevated temperatures, the model linearly extrapolates from known values.

The procedure of the tube ejection determination is as follows [5].

(1) The diameter of the tube and hole expands because the temperature of tube and hole sharply increases due to the relocated molten corium. Calculate the free thermal expansion of the tube and hole at each layer as follows.

$$\Delta r_{\mathrm{o}}^{T} = r_{\mathrm{o}}\alpha_{\mathrm{t}}\left(T_{\mathrm{t}} - T_{\mathrm{ref}}\right) \tag{6}$$

$$\Delta r_{\mathrm{h}}^{T} = r_{\mathrm{h}}\alpha_{\mathrm{h}}\left(T_{\mathrm{h}} - T_{\mathrm{ref}}\right) \tag{7}$$

where, $r_{\mathrm{o}}, r_{\mathrm{h}}, \alpha_{\mathrm{t}}, \alpha_{\mathrm{h}}$, and T_{ref} are the tube radius, the hole radius, the thermal expansion coefficient of tube and hole, the reference temperature which is 293K, respectively.

(2) Due to the pressure difference between internal reactor vessel and external reactor vessel, the tube diameter expansions. Calculate the pressure expansion of the tube at each layer as follow:

$$\Delta r_{\mathrm{o}}^{P} = \frac{\left(p_{\mathrm{i}} + p_m\right)}{E}\cdot\frac{r_{\mathrm{o}}r_{\mathrm{i}}\left(2 - \nu_{\mathrm{t}}\right)}{\left(r_{\mathrm{o}}^2 - r_{\mathrm{i}}^2\right)} \tag{8}$$

where, E and ν_t are Young's modulus of elasticity, possion's ratio which is 0.3, respectively.

The total expansion of the tube expansion is given by

$$\Delta r_o = \Delta r_o^T + \Delta r_o^P \qquad (9)$$

(3) Obtain the tube-hole radial gap(δ_i) at given the pressure and temperature ,

$$\delta_i = (r_h + \Delta r_h) - (r_o + \Delta r_o) - \delta_{clearance} \qquad (10)$$

where r_h , Δr_h , and Δr_o are the hole diameter, the total hole expansion length, and the total tube expansion length.

(4) For a locked condition, the tube-hole interface pressure that needs to be overcome in order to push out the tube is given by the lesser of the value required to make the tube conform to the final hole radius and the final hole radius and the shear stress which will cause the tube material to yield. Find tube-hole interface pressure at each layer,

$$\delta_i < 0: \; P_{th} = \text{lesser of} \left\{ \begin{array}{l} \dfrac{\delta_i \cdot E\left(r_o^2 - r_i^2\right)}{r_o\left[r_o^2(1-2\nu_t) + r_i^2(1+\nu_t)\right]} \\[2ex] \dfrac{2}{\sqrt{3}}\sigma_u \ln\left(\dfrac{r_o}{r_i}\right) \\ \text{Required pressure to cause compression} \\ \text{failure of the tube materal} \end{array} \right\}$$

$$\delta_i \geq 0: \; P_{th} = 0$$

(11)

(5) The total thermal binding shear force is calculated by summation of all incremental force.

$$V_T = \sum_{n=1}^{n} f \cdot P_{th} 2\pi r_o \Delta l_t \qquad (12)$$

where Δl_t and f are the length of the control volume and the friction factor. The frictional coefficient is not a function of temperature, but it is related to the roughness of the sliding surface. This parameter is highly variable. It could be about 0.27 for high-temperature, oxidized conditions.

(6) The ejecting pressure force is calculated by Eq. 13.

$$F_p = (p_i + p_m - p_o)\pi r_o^2$$

(13)

(7) Compare the ejecting pressure force with the total thermal binding shear force. When $F_P > V_T$, the tube ejection occurs.

When the molten corium attacks the penetration tube and the reactor vessel wall, the penetration tube and the reactor vessel wall melt due to the higher temperature of molten corium than the melting temperature. As a result, the total thermal binding shear force can decrease as the reactor vessel wall thickness decreases as time goes on ($L_t = L_t - W_{weld} t$). For the conservative model, the vessel ablation effect was considered in the modified model.

Figure 3 shows a modified calculation flow for the determination of the weld failure and the tube ejection. In this program, if the temperature of the weld, the tube, and the vessel exceeds the melting temperature after updating temperature profile, the ablation phenomena for the weld and the vessel wall were considered Furthermore, the Eq. 4 was applied to obtain the yield stress of the weld.

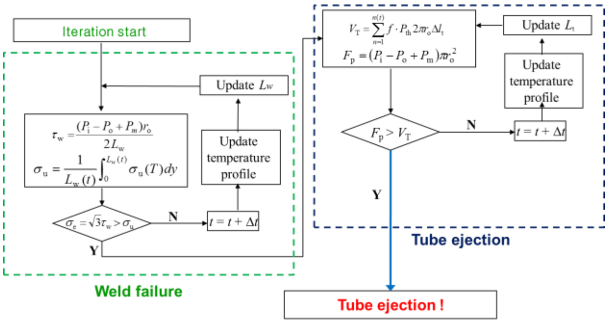

Fig. 3 Calculation steps for tube ejection model

3. Results & Discussion

3.1. Comparison with experimental result

VESTA (Verification of Ex-vessel corium STAbilization) is a facility for massive oxidic melt generation and tube ejection experiments. There are consist of two parts which are corium generation and interaction system in VESTA facility. The tube ejection experiments were performed to obtain the temperature distributions of the penetration tube, the vessel wall, and the weld [6] and to observe the tube ejection phenomena. In these tests, a material specimen in the interaction system was manufactured in accordance with the penetration tube for APR 1400 by Doosan Heavy Industries & Construction. The penetration tube is made by Inconel 690 and the reactor vessel wall is made by SA508, Grade 3, Class 1. There are 33 K-type thermocouples embedded inside the specimen for measuring the temperature distributions, specially, 4 thermocouples among 33 thermocouples embedded inside the weld region as shown in Fig. 4.

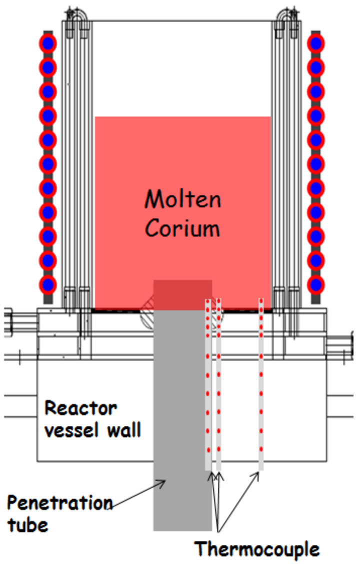

Fig. 4 Configuration of an APR 1400 penetration tube test

The melt generated at the interaction crucible which has dimensions of 280 mm in diameter and 330 mm in height. The interaction crucible was filled with ZrO_2 powder, ZrO_2 ingot, and Zr ring. In order to use the experimental results, the temperature profiles were obtained by second order least square fit (Eq.14) within the range of a discrete set of experimental data point to apply the analysis code. Since the material properties are not always available for elevated temperatures, the model linearly extrapolates from known values. The thermal properties of the SA 508 based on ASME code and the Inconel 690 for the penetration tube and the weld which is obtained from Ref. 7 were applied.

$$T(y) = a_0 + a_1 y + a_2 y^2 \qquad (14)$$

The comparison of experimental and analytic results were summarized in the Table. 1. The analytic code predicted the occurrence of tube ejection for case2, although the tube ejection did not occur at the experiment. To find this reason, the uncertainty analysis was performed.

Table 1 Comparison of experimental and analytic results

	Case1 [5]	Case2
Total mass(kg)	52.02	41.18
Composition	ZrO2 powder 99.4 wt% + Zr 0.6wt%	ZrO2 powder 99.4 wt% + Zr 0.6wt%
Maximum pressure difference	1.0 bar	2.5 bar
Experimental results		
Weld fail	Not occur	Maybe occur
Tube ejection	Not occur	Not occur
Analytic results		
Weld fail	Not occur	Occur
Tube ejection	Not occur	Occur

3.2. Uncertainty analysis

The total thermal binding shear force is a function of internal pressure, hole and tube temperature, hole radius, tube inner and outer radius, friction coefficient between the tube and hole thermal expansion coefficient, Poisson's ratios, and elastic moduli of the head and tube material. According to equations 6 to 13, the shear force has a linear relationship with these parameters. Also, the expansion direction of the tube and hole strongly effects the total thermal binding shear force. It is estimated that the sensitivity of the total thermal binding shear force to theses parameters. In order to sensitivity (uncertainty) analysis, the following assumptions were used.

- The tube-hole radial gap is 50 µm
- The pressure difference between the inside reactor vessel and the outside reactor vessel is 10 bar.
- The reactor vessel is cooled by coolant water
- The molten corium soak through a tube, so the temperature difference between internal tube wall ($T_{t,in}$) and outer tube wall ($T_{t,out}$) is 30K ($T_{t,in} - T_{t,out} = 30$) [4]
- The vessel temperature has a linear profile, and the ratio of the internal vessel wall temperature ($T_{h,in}$) to the outer vessel wall temperature ($T_{h,out}$) is constant, such as $\frac{T_{h,out}}{T_{h,in}} = c$. 0.73 were used for the constant value.

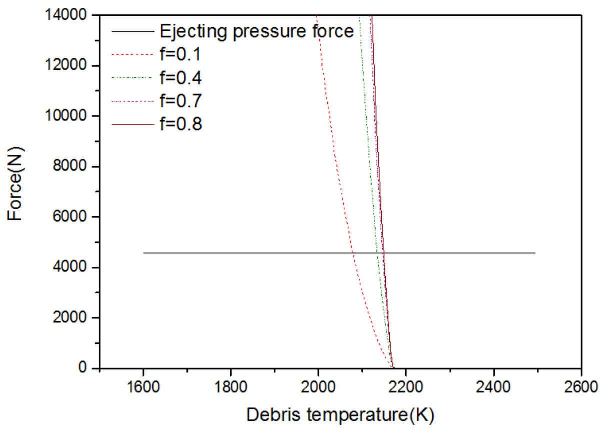

Fig. 5 Effect of the friction factor to the tube ejection

The frictional coefficient is not a function of temperature, but it is related to the roughness of the sliding surface. This parameter can be highly variable, but it was assumed to be about 0.27. It was found that the debris temperature which leads to the tube ejection with various friction factor values. The tube ejection force doesn't change due to no change in the pressure difference and the area, as shown in Fig. 5. When the friction factor changed from 0.1 to 0.8, the tube ejection temperature is changed from about 2080 °C to 2150 °C.

There are some uncertainty in the ultimate strength and elastic modulus of the tube material and coefficients of thermal expansion of the tube and vessel which vary significantly with temperature, to be used at these high temperature. The model linearly extrapolates from known values for the high temperature. For example, the ultimate strength are extrapolated linearly to zero at the melting temperature for the highest known temperature data. The effect of the uncertainty of these parameters on the thermal binding shear force is similar to the effect of the uncertainty of the friction factor because the thermal binding shear force has a linear relationship with them. It is known that the strength data could vary enough to result in an uncertainty band of 200 K about the tube failure [4].

In the weld failure mechanism, the weld failures occur as a result of the ultimate strength reducing which is lower than pressure-induced stresses due to the higher temperatures as shown Eq. 4. So, it is estimated that the weld thickness and the debris temperature at the occurrence of weld failure as the change of the ultimate strength. The effective stress increases as the debris temperature increases due to the decrease in the weld thickness as shown in Fig. 6. When the ultimate strength is decreased by 40% from Ref. [7], it is observed that the debris temperature to occur weld fail is changed about 10°C which is from 1730°C to 1740°C and the weld thickness changed from 2 mm to 8 mm.

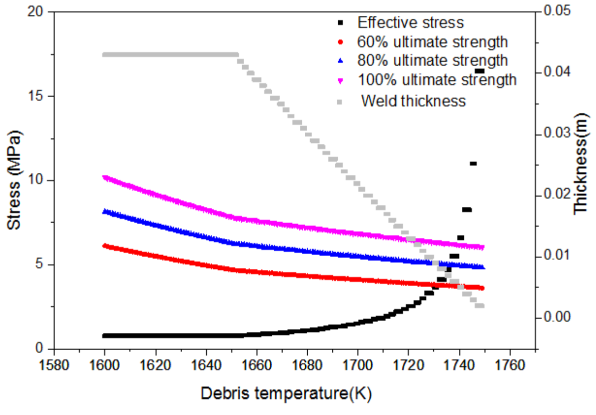

Fig. 6 Effect of the ultimate strength to the weld failure

Although theses parameters can be strongly affected to the analytic results, there is still the difference between experimental results and the analytic results. So, it is also investigated that the effect of the expansion direction of the tube and hole on the total thermal binding shear force. The expansion direction of the tube and hole differs at the penetration tube location of the lower head. Although the Eq. (10) is the most conservative assumption to determine the failure mode, in order to investigate the effect of the expansion direction of the tube and hole, Eq. (15) was applied instead of Eq. (10) in the procedure of the tube ejection determination.

$$\delta_i = (r_h - \Delta r_h) - (r_o + \Delta r_o) - \delta_{clearance} \qquad (15)$$

In this case, when the tube and the vessel temperature is higher than 1000K, the tube-hole radial gap is always less than zero. This means that the incremental surface area of the interface leading to an incremental friction force. Furthermore, the analytic results match well with the experimental results.

It is indicated that uncertainties in analytic results are primality attributed to uncertainty in the expansion direction of the tube and the hole and the study of the expansion direction of the tube and the hole in VESTA facility is required to compare the analytic model. Also, to get higher prediction for failure mode, the more validation work is required against the experimental data which observe the tube ejection with various conditions such as with or without the ex-vessel reactor vessel cooling.

4. Conclusion

The failure model in the severe accident code requires a large amount of effort to increase the prediction of failure mode. The brief description of the modified failure models considered both the thermal and structural response of the vessel and lower head penetrations, along with assumptions used in the models, is provided. The code validation works were performed based on the VESTA experimental results. The uncertainty analysis was also performed because there is the difference between the analytic results and the experimental results. It was found that uncertainties in analytic results are primality attributed to uncertainty in the expansion direction of the tube and the hole. For reasonable estimation of the failure mode, the study of the expansion direction of the tube and the hole in VESTA facility is required. Furthermore, more experimental data with various boundary conditions such as the ex-vessel reactor vessel cooling is required to improve the failure model, which left as a future work.

ACKNOWLEDGMENTS

This work was supported by the National Research Foundation of Korea (NRF) grant funded by the Korea government (MSIP) (No. 2012M2A8A4025885).

REFERENCES

[1] B. R. Sehga, Nuclear Safety in Light Water Reactors-Severe Accident Phenomenology, Academic Press, Boston, 2012.
[2] Report of Japanese Government to the IAEA Ministerial Conference on Nuclear Safety - The Accident at TEPCO's Fukushima Nuclear Power Stations -, June 2011, Nuclear Emergency Response Headquarters, Government of Japan.
[3] MAAP5 Code Manual, Fauske & Associates, Inc, 2008.
[4] J.L.Rempe, S.A. Chavez, G.L. Thinnes et.al., Light Water Reactor Lower Head Failure Analysis, EG&G Idaho, NUREG/CR-5642 EGG-2618, October, 1993.
[5] J. Jung, S. M. An, K.S. Ha, H. Y. Kim, Assessment of penetration failure for APR 1400, Proceedings of 2015 International Conference on the Advances in Nuclear Power Plants (ICAPP 2015), May 03-06, 2015, Nice, France.
[6] S. M. An, J. Jung, K.S. Ha, H. Y. Kim, Experimental investigation on APR1400 in-core instrumentation penetration failure during a severe accident, Proceedings of 2015 International Conference on the Advances in Nuclear Power Plants (ICAPP 2015), May 03-06, 2015, Nice, France.
[7]http://www.specialmetals.com/documents/Inconel%20alloy%20690.pdf